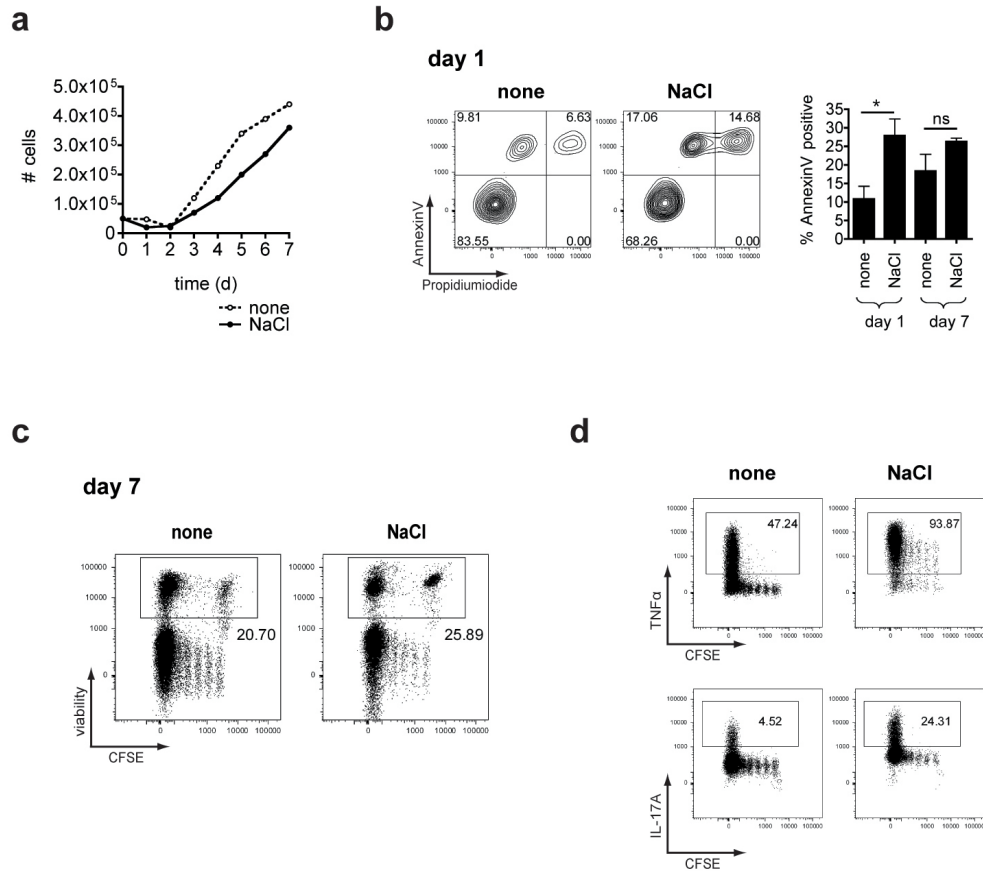
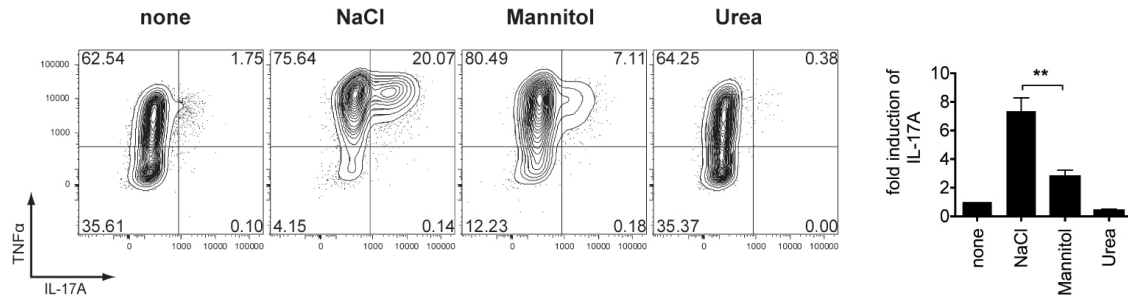


Supplementary Figure 1 | Cytokine requirements for optimal Th17 cell induction under high-salt conditions. Naïve human CD4⁺ T cells were stimulated with anti-CD3 and anti-CD28 and the indicated cytokines in the presence or absence of additional 40mM NaCl. Data is representative of three independent experiments.

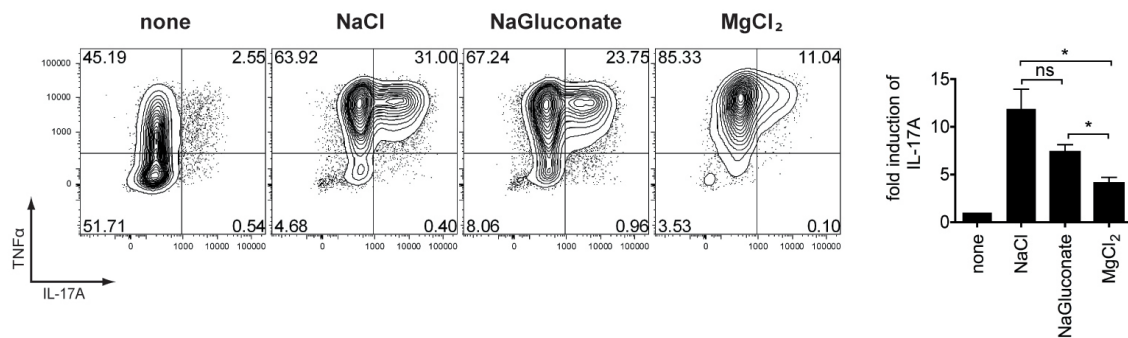


Supplementary Figure 2 | Effect of increased NaCl on proliferation and viability of human T cells. Naïve human CD4⁺ T cells were cultured in normal medium or medium containing additional 40mM NaCl and stimulated with anti-CD3 and anti-CD28 in the presence of IL-1 β , IL6, IL21, IL23 and TGF- β 1. **a**, Absolute cell numbers were determined daily by counting the cells under a microscope using a viability stain (n=2). **b**, Frequencies of AnnexinV positive cells and dead cells were determined on day 1 and day 7 by FACS (n=3). The left panel depicts a representative staining at day 1. **c**, The number of cell divisions and percentage of dead cells at day 7 was visualized by CFSE-dilution and a viability stain. **d**, Representative intracellular staining of TNF α (upper row) and IL-17A (lower row) against CFSE on day 7.

a

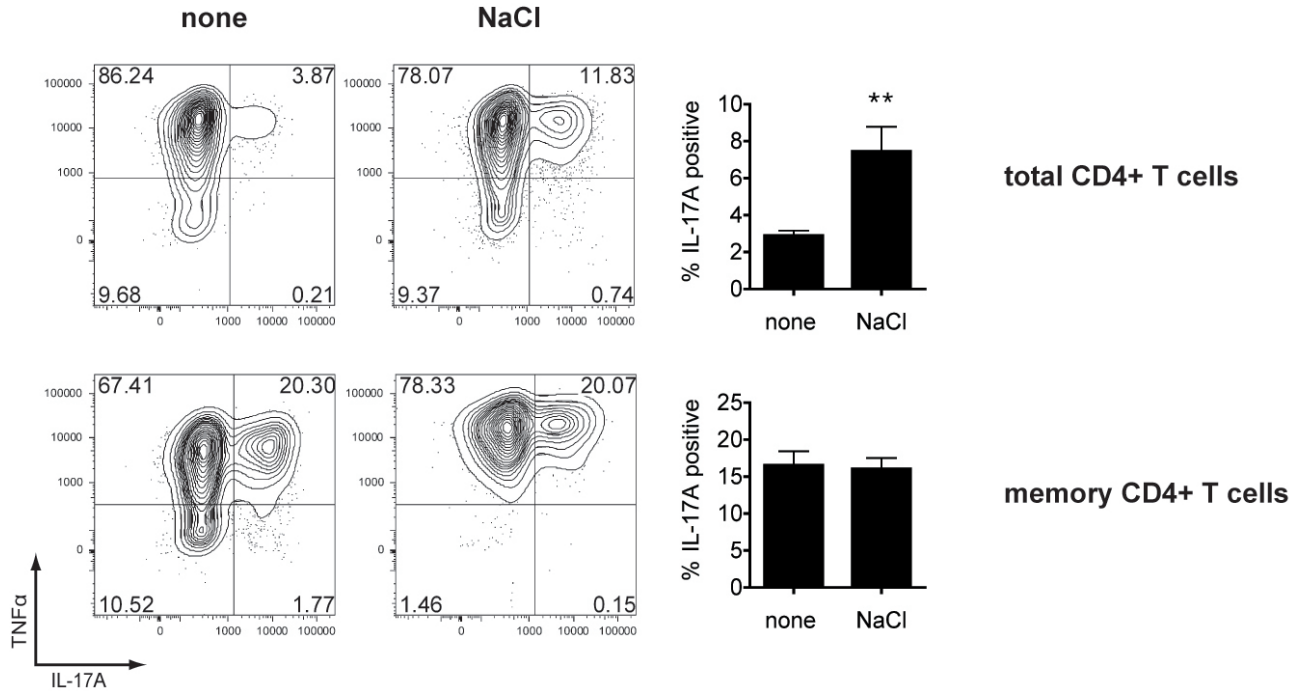


b

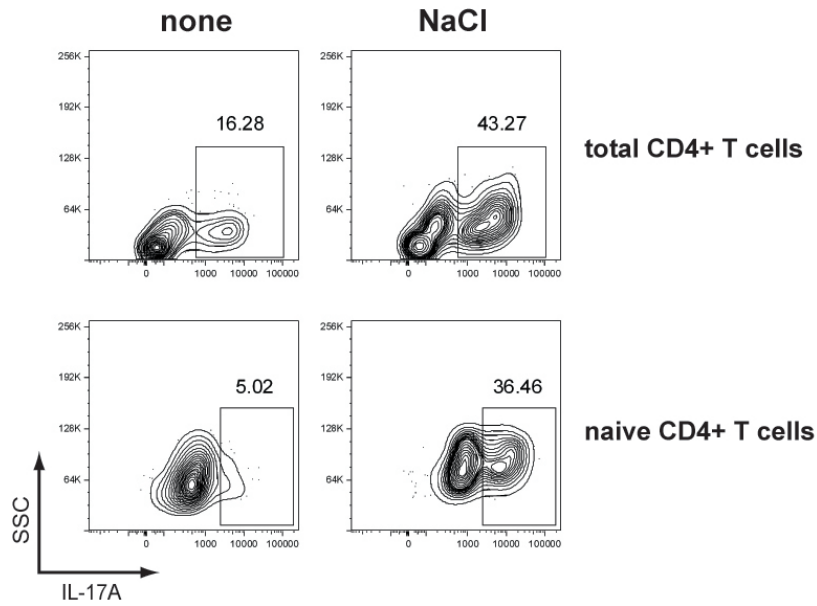


Supplementary Figure 3 | Effects of various stimuli on the Th17 cell induction in human T cells.

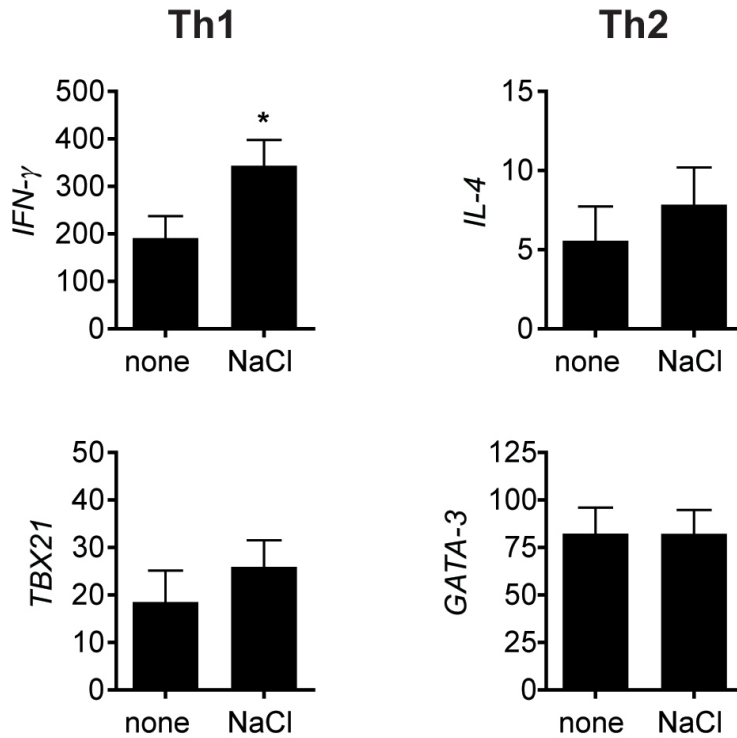
a, Naïve human CD4⁺ T cells were stimulated with anti-CD3, anti-CD28, IL-1β, IL-6, IL-21, IL-23 and TGF-β1 in the absence or presence of additional 40mM NaCl, 80mM mannitol or 80mM urea and were analysed by FACS for the expression of IL-17A and TNFα. A summary of IL-17A expression is shown in the bar graph (normalised to controls, n=6-8). **b**, Naïve T cells were stimulated as in a), in the presence or absence of additional 40mM NaCl, 40mM sodium gluconate or 26.7mM MgCl₂ and analysed by FACS as in a). A summary of IL-17A expression is shown in the lower panel (normalised to controls, n=4).



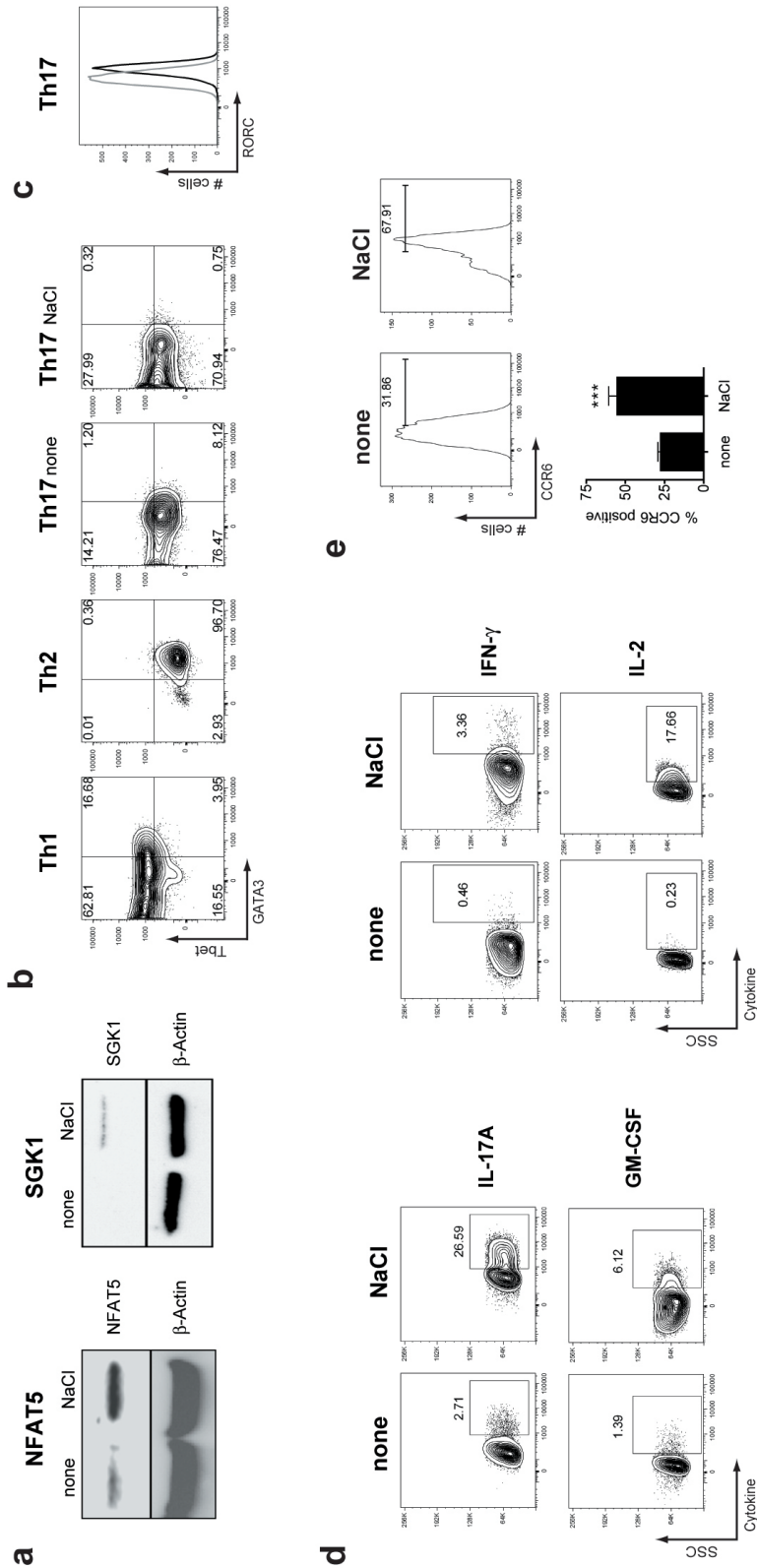
Supplementary Figure 4 | Consequences of increased NaCl on Th17 induction in total and memory CD4⁺ T cells. Total human CD4⁺ T cells (upper panel) or memory CD4⁺ T cells (lower panel) were stimulated with anti-CD3, anti-CD28, IL-1 β , IL-6, IL-21, IL-23 and TGF- β 1 in the presence or absence of additional 40mM NaCl and were analysed by FACS for IL-17A and TNF α expression. A summary of IL-17A expression determined by FACS is shown in the right panels (n=6).



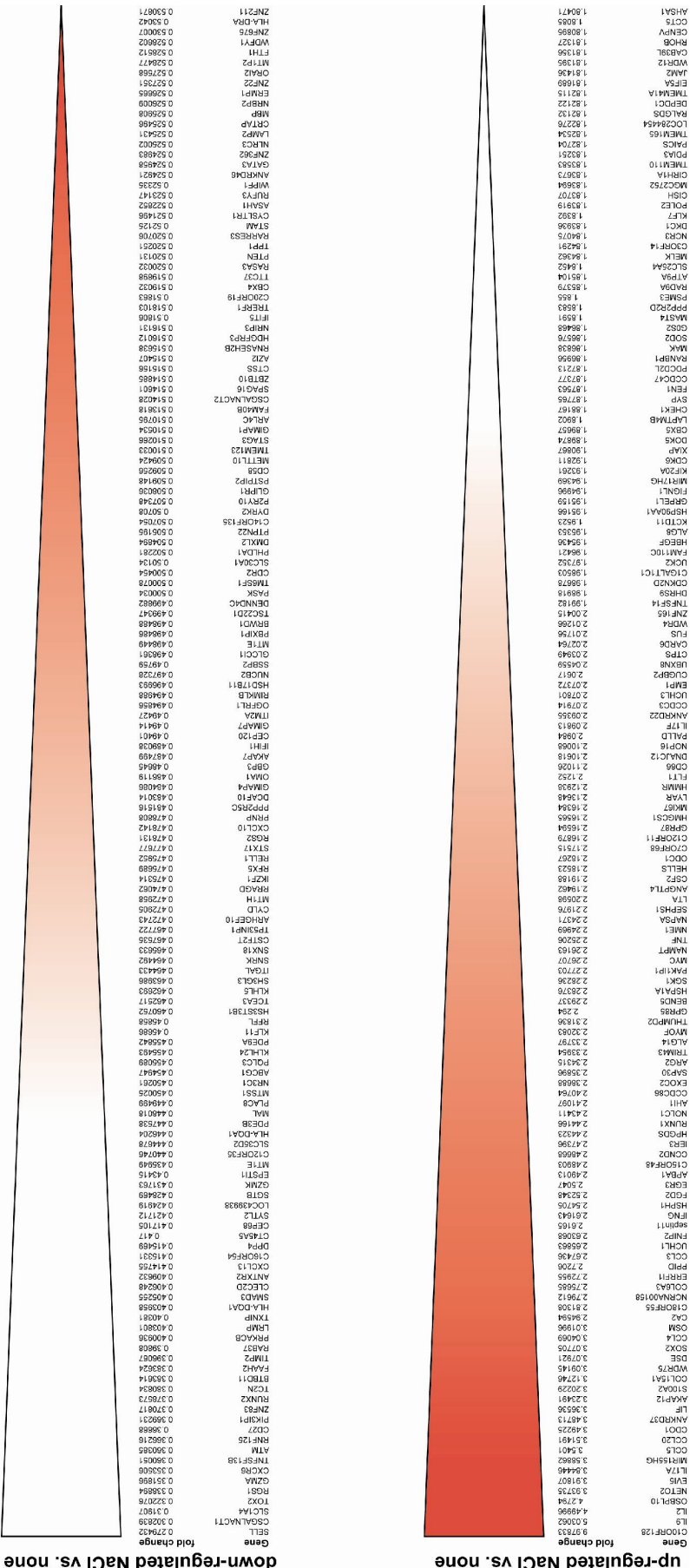
Supplementary Figure 5 | Antigen specific activation of CD4⁺ T cells under high-salt conditions. Total human CD4⁺ T cells (upper panel) or naive CD4⁺ T cells (lower panel) were cultured with *candida albicans* pulsed autologues CD14⁺ monocytes in the presence (right panels) or absence (left panels) of additional 40mM NaCl and were analysed by FACS for IL-17A expression. Data is representative of two independent experiments.



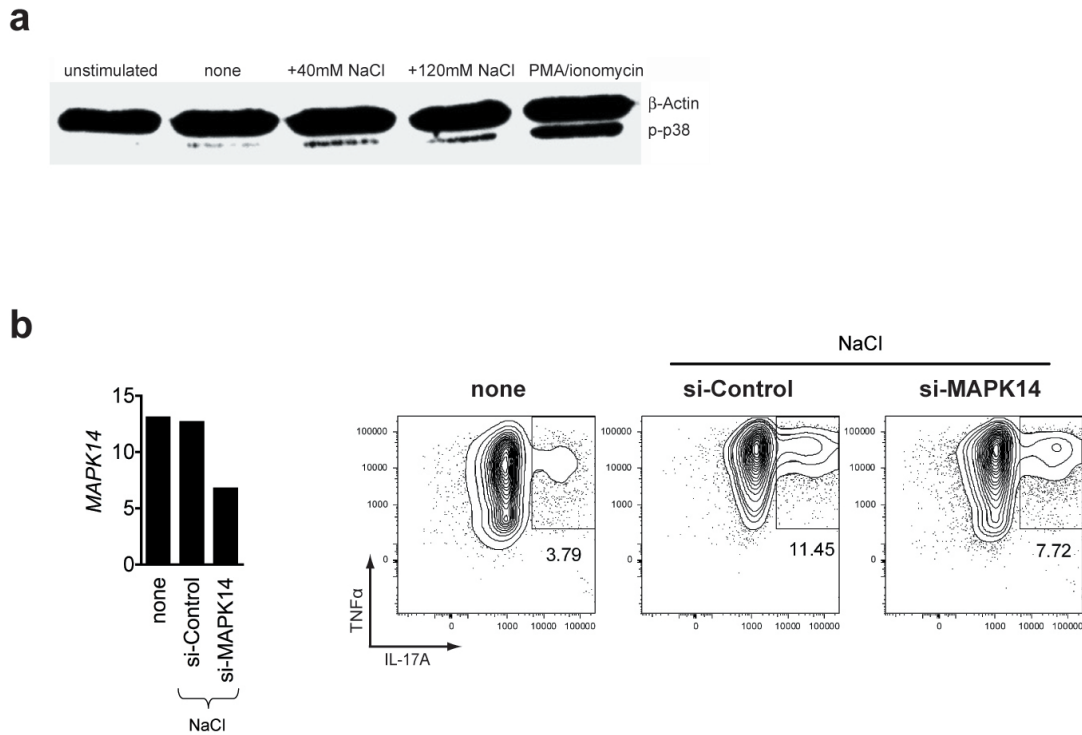
Supplementary Figure 6 | Consequences of increased NaCl on Th1 and Th2 differentiation in human T cells. Naive human CD4⁺ T cells were stimulated with anti-CD3 and anti-CD28 in the presence of IL-12 and anti-IL-4 for Th1 differentiation (left panel) or IL-4 and anti-IFN- γ for Th2 differentiation (right panel) under normal (none) or high-salt (NaCl) conditions. mRNA expression was analysed by qRT-PCR for *IFN- γ* and *Tbet* (Th1 cells) and *IL-4* and *GATA-3* (Th2 cells) (n=5-8).



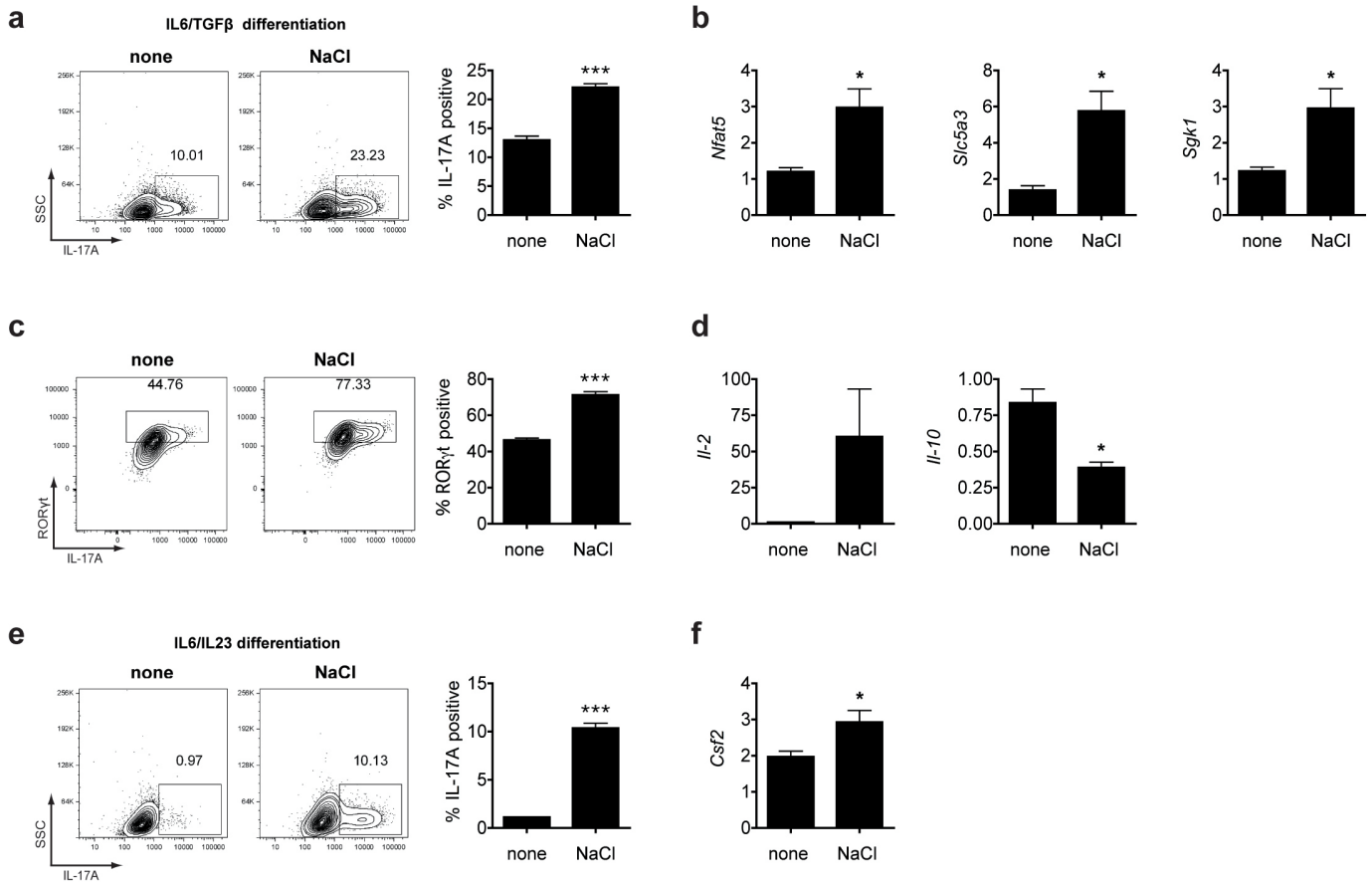
Supplementary Figure 7 | Characterisation of high-salt induced Th17 cells. Naive human CD4⁺ T cells were stimulated with anti-CD3, anti-CD28, IL-1 β , IL-6, IL-21, IL-23 and TGF- β 1 in the presence (NaCl) or absence (none) of additional 40mM NaCl. **a**, Western blot analysis of NFAT5 (left panel) and SGK1 (right panel) in comparison to β -Actin. Data is representative of two independent experiments. **b**, FACS analysis of Tbet and GATA3 expression on Th1, Th2 and Th17 cells. Data is representative of four independent experiments. **c**, FACS analysis of RORC expression on Th17 cells differentiated in the absence (grey line) or presence (black line) of additional 40mM NaCl. Data is representative of four independent experiments. **d**, Analysis of cytokine expression by FACS. Data is representative of four independent experiments. **e**, Analysis of CCR6 expression on Th17 cells by FACS (n=6).



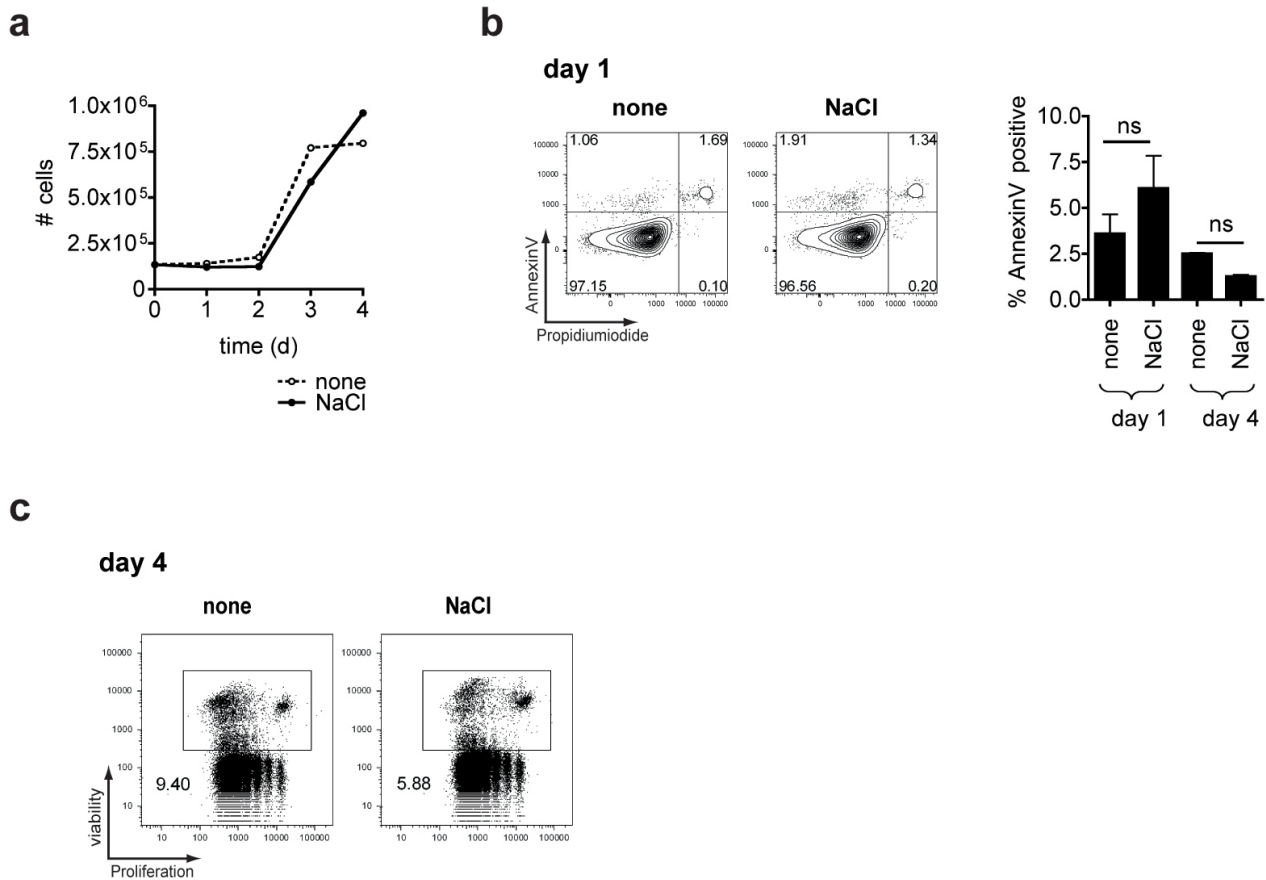
Supplementary Figure 8 | Microarray analysis of Th17 cells generated in the presence or absence of additional 40mM NaCl. Naïve human T cells from two donors were stimulated with anti-CD3, anti-CD28, IL-1 β , IL-6, IL-21, IL-23 and TGF- β 1 in the presence or absence of additional 40mM NaCl. Total RNA was isolated and subjected to microarray analysis. The list shows the 150 highest up- (left panel) and down-regulated (right panel) genes (fold change represents mean values of the two analysed donors).



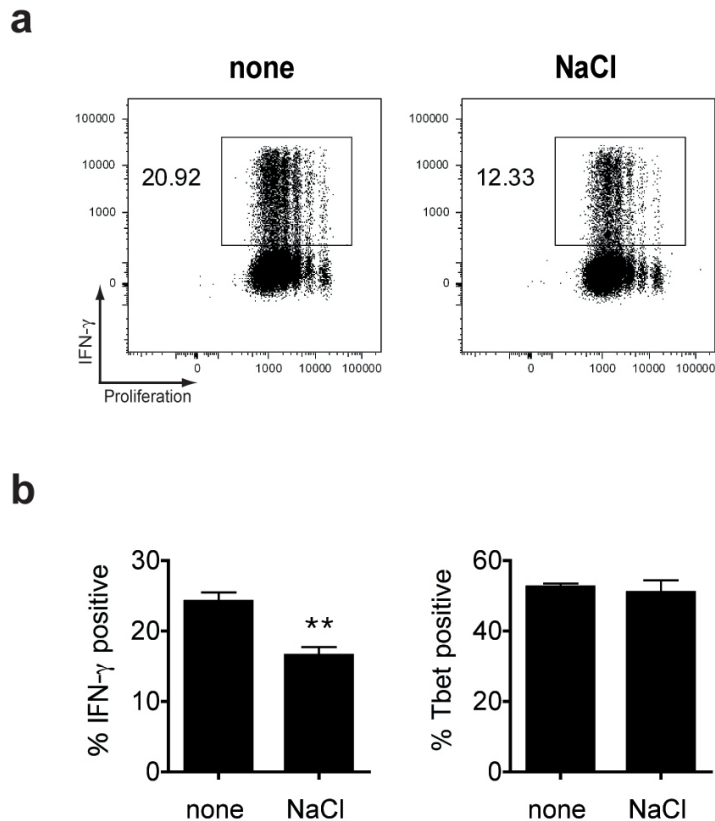
Supplementary Figure 9 | p38/MAPK is critical for high-salt mediated Th17 induction in humans. **a**, Western blot analysis for phospho-p38 of human CD4⁺ T cells in comparison to β -Actin. Cells were stimulated for 20 min. with anti-CD3, anti-CD28, IL-1 β , IL-6, IL-21, IL-23 and TGF- β 1 in the presence of increasing NaCl concentrations or PMA/ionomycin as indicated. Data is representative of two independent experiments. **b**, siRNA knockdown of *MAPK14* in CD4⁺ T cells. Cells were transfected by electroporation with siRNA specific for *MAPK14* or nonspecific siRNA and stimulated with anti-CD3, anti-CD28, IL-1 β , IL-6, IL-21, IL-23 and TGF- β 1 in the presence of additional 40mM NaCl. mRNA expression of *MAPK14* was analysed on day 3 (left panel) and IL-17A and TNF α protein expression was analysed by FACS after 6 days (right panels). Data is representative of two independent experiments.



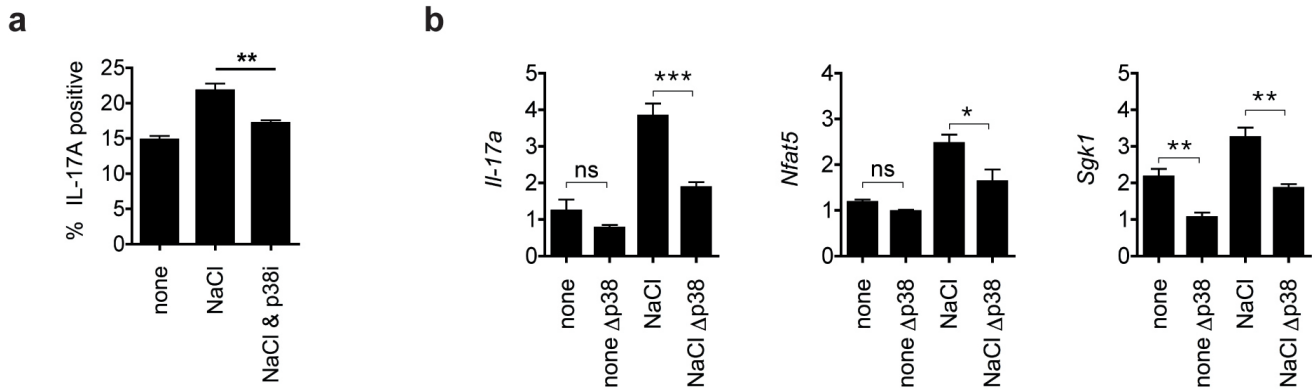
Supplementary Figure 10 | Phenotype of murine Th17 cells induced under various conditions *in vitro*. Naïve murine CD4⁺ T cells were cultured in normal medium or medium containing additional 40mM NaCl and stimulated for 96h with anti-CD3 and anti-CD28 in the presence of TGF- β 1 and IL-6 (a-d) or IL-23 and IL-6 (e, f). Frequencies of IL-17A positive (a, n=11) and ROR γ t positive (c, n=4) cells were determined by FACS. RNA was isolated after 96h and mRNA expression was measured by qRT-PCR for the indicated genes (b, d, n=3; f n=5).



Supplementary Figure 11 | Effect of increased NaCl on proliferation and viability of murine T cells. Naïve murine CD4⁺ T cells were cultured in normal medium or medium containing additional 40mM NaCl and stimulated with anti-CD3 and anti-CD28 in the presence of TGF-β1 and IL-6. **a**, Absolute cell numbers were determined daily by counting viable cells on a flow cytometer using true-count beads (n=3). **b**, Frequencies of AnnexinV positive cells and dead cells were determined on day 1 and day 4 by FACS (n=3). The left panel depicts a representative staining at day 1. **c**, The number of cell divisions at day 4 was visualized by dye-dilution and a viability stain.

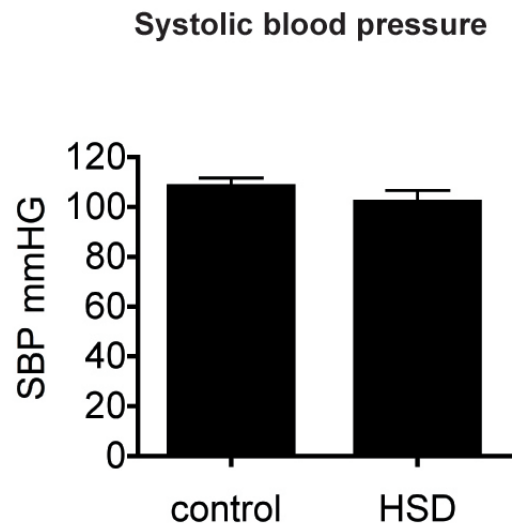


Supplementary Figure 12 | Consequences of increased NaCl on Th1 development in murine T cells. Naïve murine CD4⁺ T cells were cultured in normal medium or medium containing additional 40mM NaCl and stimulated for 96h with anti-CD3, anti-CD28, IL-12 and anti-IL-4. **a**, Cell divisions, as determined by dye-dilution and intracellular production of IFN- γ were analysed simultaneously by FACS. **b**, The left panel shows the percentage of IFN- γ positive cells as measured like in a, (n=6). The frequency of Tbet positive cells was determined by intracellular staining (right panel, n=4).

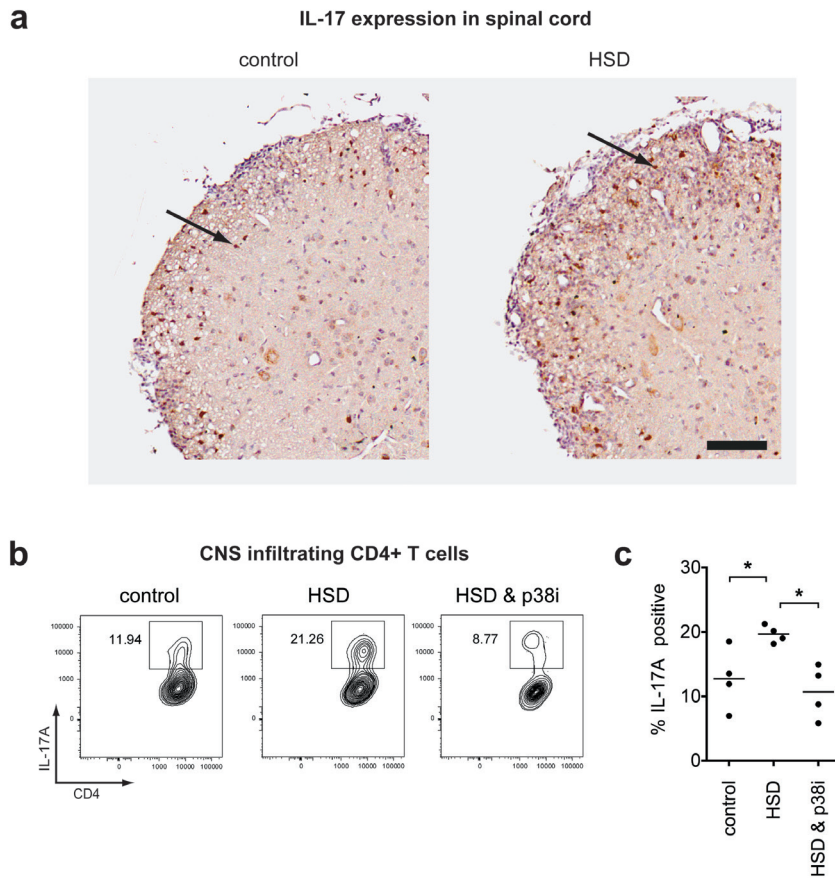


Supplementary Figure 13 | p38/MAPK is involved in high-salt mediated Th17 induction in mice.

Naïve murine CD4⁺ T cells were cultured in the presence or absence of additional 40mM NaCl and stimulated for 96h with anti-CD3, anti-CD28, TGF- β 1 and IL-6. Frequencies of IL-17A positive cells were determined by intracellular flow cytometry or qRT-PCR. **a**, Blockade of p38/MAPK by SB202190 (p38i) reverses the high-salt mediated IL-17A induction (n=6). **b**, Naïve T cells from Mx-Cre⁺ p38 α ^{*fl/fl*} mice were stimulated under Th17 conditions as indicated above and mRNA was analysed by qRT-PCR for *Il-17a*, *Nfat5* and *Sgk1* (n=6).



Supplementary Figure 14 | Blood pressure of animals fed a control or high-salt diet. The Systolic blood pressure (SBP) of animals fed a control or high-salt diet (HSD) was measured by tail-cuff on day 18 post induction of EAE and is displayed as mmHg (n=5).



Supplementary Figure 15 | Characterisation of IL-17 expression in CNS and spinal cord infiltrating cells of EAE animals and *in vivo* blockade of p38/MAPK. **a**, Lumbar spinal cord sections of animals on a control or high-salt diet (HSD) were prepared at day 20 p.i. of EAE and stained with antibodies against IL-17 (scale bar= 100 μ M, data is representative of three mice, arrows indicate IL-17⁺ cells). **b**, Mice were maintained on a control or HSD. For inhibition of p38/MAPK, mice were injected with SB202190 (p38i). Brain leukocytes were isolated on day 17 p.i. of EAE and analysed by FACS for IL-17A and CD4 after stimulation with PMA/ionomycin. One representative staining is shown for each group. **c**, The dotplot depicts the percentage of IL-17A⁺ cells of individual mice in each group, mean values are indicated by the horizontal lines (n=4).